ELSEVIER

Thin Solid Films 377–378 (2000) 803–808

thin solid films

www.elsevier.com/locate/tsf

Growth of epitaxial doped strontium sulfide thin films by pulsed laser deposition

A. Piqué[a,*], R.C.Y. Auyeung[a], S.B. Qadri[a], H. Kim[b], B.L. Justus[a], A.L. Huston[a]

[a] *U.S. Naval Research Laboratory, 4555 Overlook Avenue, S.W., Washington, DC 20375, USA*
[b] *School of Engineering and Applied Science, George Washington University, 725 23rd Street, N.W., Washington, DC 20052, USA*

Abstract

Epitaxial luminescent thin films of doped strontium sulfide (SrS) have been grown using pulsed laser deposition (PLD). SrS films double doped with Eu and Sm, Ce and Sm and Cu and Ge were deposited with thicknesses ranging from 0.05 to 2 μm on MgO(001) substrates. Optical microscopy, scanning electron microscopy (SEM) and atomic force microscopy (AFM) analysis were used to study the films' surface morphology. The PLD-grown films were highly oriented as determined by their X-ray diffraction (XRD) spectra and showed signs of little or no strain, and very low lattice mismatch when deposited on MgO. The best results were obtained for films deposited between 750 and 800°C and under H_2S background pressures ranging from 10 to 20 mtorr. The thermally-stimulated luminescence properties of these films were evaluated as well. The data indicate that these films would be well-suited for display applications. © 2000 Elsevier Science B.V. All rights reserved.

Keywords: Strontium sulfide thin films; Epitaxial; Pulsed laser deposition; SrS:Eu,Sm; SrS:Ce,Sm; SrS:Cu,Ge

1. Introduction

Among the numerous types of phosphor compounds available, doped alkaline-earth sulfides have been employed extensively due to their high luminescent yields. In thin film form, these materials offer great potential for applications such as infrared sensors and X-ray radiation imaging plates [1], optical storage media [2], and electroluminescent (EL) displays [3,4]. Because of their great commercial impact, both optical storage and EL display applications have been explored by numerous groups and each presents numerous challenges for materials development. Among the numerous II–VI compounds used as phosphor hosts, strontium sulfide (SrS) is often chosen due to its large bandgap ($E_g > 4$ eV), which allows it to emit visible light without self-absorption. The luminescent properties of the phosphor; however, are determined by the dopants introduced in the host lattice. Rare earths such as Eu, Tb, Pr and Ce, or metals such as Cu, are commonly used as dopants in SrS.

Phosphor materials in thin film form offer significant advantages over conventional bulk powders for display applications, such as higher resolution, more uniform density and increased thermal stability. However, current polycrystalline thin film phosphors exhibit noticeably lower luminescent output than their powder counterparts [5]. It appears that the greatest challenge in the processing of sulfur-based phosphors in thin film form is the incorporation of the dopants with the correct charge state uniformly within the host lattice. Deficient stoichiometry and poor crystallinity of the host lattice have also been found to affect the films luminescent properties [6].

SrS:Eu,Sm is an orange luminescent phosphor (caused by excitations from the Eu^{2+} ions), while SrS:Ce,Sm is a blue phosphor (caused by excitations from the Ce^{3+} ions). In both these materials, the Sm^{2+}

* Corresponding author. Tel.: +1-202-767-5653; fax: +1-202-767-5301.
E-mail address: pique@nrl.navy.mil (A. Piqué).

0040-6090/00/$ - see front matter © 2000 Elsevier Science B.V. All rights reserved.
PII: S0040-6090(00)01294-3

serves as a source of electron traps, which makes them attractive candidates for optical storage applications [7]. SrS doped with Cu and Ge (the Ge ions are used for charge compensation) is a blue luminescent phosphor with superior chromaticity than that of SrS:Ce, which has attracted considerable attention recently due to its potential application for the fabrication of full-color electroluminescent displays [8,9]. In this work, the growth of epitaxial, highly uniform double doped SrS films using pulsed laser deposition (PLD) was studied. Highly oriented SrS:Eu,Sm, SrS:Ce,Sm and Sr:Cu,Ge films were deposited on MgO substrates under a wide range of temperatures and H_2S background pressures. The structure of the SrS host and the films surface morphology were evaluated as a function of the growth parameters. The thermally stimulated luminescent properties of SrS:Eu,Sm and SrS:Ce,Sm films were measured also.

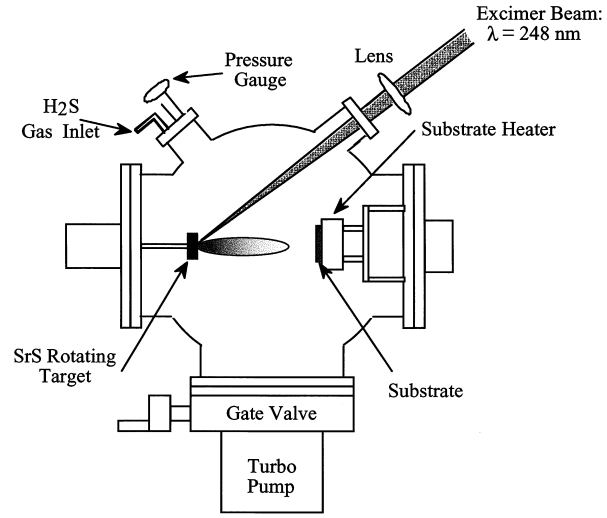

Fig. 1. Schematic of the PLD system used for this work.

2. Experimental details

2.1. Thin film fabrication

The films prepared for this work were deposited inside a conventional pulsed laser deposition system and a KrF excimer laser (30 ns pulse length at 248 nm) was used. The MgO substrates employed were (001)-oriented, double-side polished single crystal slabs, 1 cm × 1 cm by 0.05 cm thick. The SrS:Eu,Sm, SrS:Ce,Sm and SrS:Cu,Ge targets used for this work were ≈ 5.0 cm in diameter by 0.6 cm thick and their density was determined to be over 85% of the theoretical density for SrS. Due to their high density, these targets were expected to yield virtually particle-free films by PLD.

Fig. 1 shows a schematic of the PLD system utilized in this work. The excimer laser beam was incident on the target at a 45° angle and was focused onto a spot 0.1 cm^2 in area. The laser fluence at the target was adjusted between 1 and 2 J/cm^2. During depositions, the laser was fired at 5 Hz and the beam rastered over a portion of the rotating target. Under these conditions, deposition rates of 2.5 Å/s resulted in SrS films 0.05–2.0 μm thick over the MgO substrates. The SrS films were deposited under H_2S partial pressures varying from 0.1 to 200 mtorr, and at temperatures ranging from 600 to 850°C. At the end of each deposition, the films were allowed to cool in a mixture of 1 torr of H_2S and 500 torr of Ar.

2.2. Thin film characterization

The film thickness was measured using a stylus profilometer (Tencor Alpha-Step 250). The surface morphology of the films was first evaluated using optical microscopy. Several samples were selected for further analysis using a LEO-1500 Scanning Electron Microscope and a Digital Instruments Dimension 3100 Atomic Force Microscope.

The structure of the SrS films was studied using a two-circle diffractometer (Rigaku Rotaflex, with CuKα radiation) for analysis of the out-of-plane orientation of the epitaxial films. In order to determine the in-plane alignment of the films, azimuthal scans were performed using a Huber four circle diffractometer and CuKα radiation from a Rigaku rotating anode source. For the azimuthal scans, a graphite crystal was used to select the $CuK\alpha_{1,2}$ radiation and the $CuK\alpha_2$ component was eliminated by adjusting the width of the slits on the exit side of the monochromator. The experimental broadening as measured by the reflection from the MgO(002) and (004) substrate peaks was 0.145° in 2θ which is essentially the angular divergence of the incident CuKα radiation.

The thermally stimulated luminescence (TSL) properties were evaluated as well using a Harshaw/Bicron 3500 thermoluminescence dosimetry (TLD) reader with a 600-nm cut-off filter for blocking the black-body radiation. The TSL measurements were performed on 0.5 cm × 0.5 cm sections diced from the larger samples so they would fit inside the heated stage of the TLD reader.

3. Results and discussion

The surface quality of the SrS films was first evaluated using optical microscopy. No particulates or outgrowths, often associated with PLD films were detected. Both the SrS:Eu,Sm and SrS:Cu,Ge films exhibited very smooth surfaces as observed under the optical microscope. However, the SrS:Ce,Sm films showed very large grain-like features on their surfaces ranging in size from 2 to 10 μm in diameter, independent of the growth conditions. The spacing between grains aver-

aged approximately 5 μm. Despite this, the regions between these grains were quite uniform. These initial observations were later confirmed when the films were evaluated using SEM and AFM. For the SrS:Eu,Sm films, SEM analysis showed their surface to be quite uniform, free of voids or cracks, all indicative of a high quality film. At high magnifications (30 000 ×) the films reveal a fine structure, with ≈ 200-nm grain-like features as shown in Fig. 2a. For the SrS:Ce,Sm films, SEM analysis confirmed the observations made with the optical microscope. The shape of the grains was highly regular with diameters of approximately 5 μm. Because of their uniform shape, it is very unlikely that these grains originated from particulates ejected during the ablation of the target. The cause for these structures present in every SrS:Ce,Sm film deposited in this work is not yet clear. In between the boulders, the film surface was quite uniform, as shown in Fig. 2b. The SrS:Cu,Ge films appeared very uniform under the SEM; however, the presence of void-like features could be observed, see Fig. 2c.

The above films were also evaluated by AFM. Fig. 3a shows an image from a 2 μm × 2 μm region near the center of the SrS:Eu,Sm film. Grain-like structures, ≈ 300 nm in size can be observed, in good agreement with the features observed with the SEM. The root-mean-square (rms) surface roughness for this film is 2.3 nm, which is rather good if compared with that of SrS:Eu,Sm films deposited by sputtering, where typical rms surface roughness are approximately an order of magnitude larger [10]. For the SrS:Ce,Sm films, AFM analysis showed the boulder structures to average several micrometers in height or several times the film thickness. In between, however, the resulting film is relatively uniform, with rms surface roughness of 9.9 nm, see Fig. 3b. The SrS:Cu,Ge films show rms surface roughness of 7.9 nm, with a uniform distribution of grains ≈ 200 nm in size.

The SrS host, with its sodium chloride cubic structure ($a = 6.022$ Å), is expected to grow epitaxially over

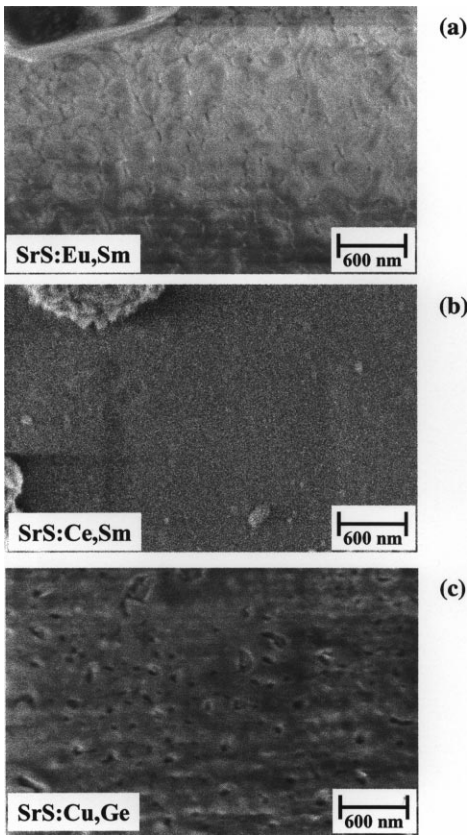

Fig. 2. SEM images belonging to the three differently doped SrS thin films deposited for this work. (a) SrS:Eu,Sm; (b) SrS:Ce,Sm and (c) SrS:Cu,Ge.

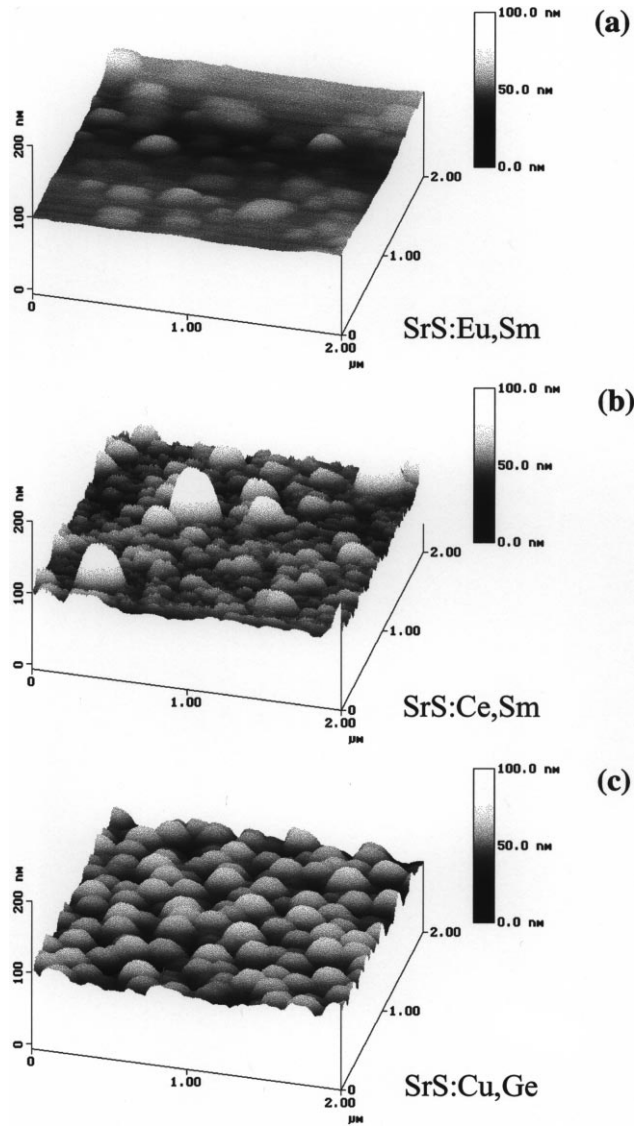

Fig. 3. AFM images (2 μm × 2 μm) belonging the three types of doped SrS thin films deposited for this work. (a) SrS:Eu,Sm, rms surface roughness of 2.3 nm. (b) SrS:Ce,Sm, rms surface roughness of 9.9 nm. (c) SrS:Cu,Ge, rms surface roughness of 7.9 nm.

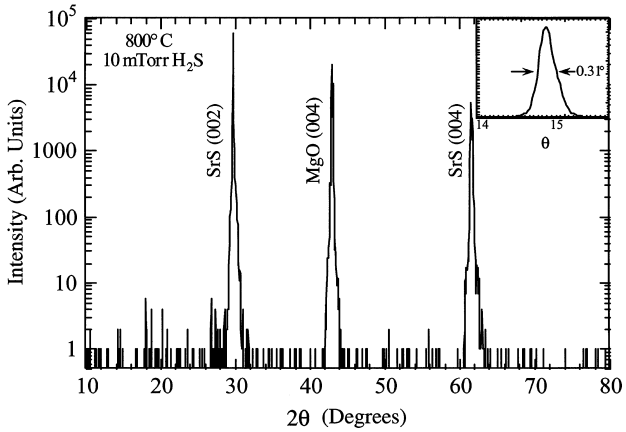

Fig. 4. XRD spectra for a SrS:Eu,Sm film grown on an MgO(001) substrate at 750°C and in 20 mtorr of H_2S. Insert shows the rocking curve belonging to the (002) SrS peak.

the MgO(001) substrates ($a = 4.213$ Å), given the appropriate deposition conditions. The X-ray diffraction (XRD) spectra of the numerous films produced in this work confirmed this. MgO was chosen due to the fact that it provides a good template for SrS to grow epitaxially and does not react chemically with the SrS film during its growth [11]. The preferred film growth orientation was confirmed by the θ−2θ XRD scans, which revealed the SrS films grew only along the (001) direction. Only peaks belonging to the SrS (001) and MgO (001) families of planes were observed, indicating that no significant amount of undesired phases generated by chemical reactions between the substrate and the film were formed. Fig. 4 shows a typical θ−2θ XRD scan for a SrS:Eu,Sm film deposited on a MgO substrate at 800°C and in 20 mtorr of H_2S. The θ−2θ scans belonging to the SrS:Ce,Sm and SrS:Cu,Ge films were essentially identical. The insert in Fig. 4 shows the rocking curve belonging to the (002) peak from this film.

Previous work by this group indicated that the full width at half maximum (FWHM) of the X-ray rocking curves from the SrS (002) reflection ($2\theta \approx 29.7°$) can be used as an optimization parameter for the film growth conditions [11]. By adjusting the temperature and H_2S pressure during deposition, it was possible to minimize the FWHM values. For the SrS:Eu,Sm films, their FWHM showed a minima for the films deposited between 750 and 800°C and between 10 and 20 mtorr of H_2S. For the SrS:Ce,Sm and SrS:Cu,Ge films, the narrowest FWHM values were obtained for those films deposited at 750 and 800°C, respectively, and in 10 mtorr of H_2S.

The measured FWHM of the (002), (004) and (006) SrS reflections were used to estimate the average strain in the SrS/MgO peaks. After correcting for the instrumental broadening, which was calculated from the (002) and (004) substrate reflections, the corrected FWHM were fitted to the following equation:

$$\beta_c^2 = K_\alpha + K_\varepsilon \tan^2\theta \quad (1)$$

where β_c is the corrected FWHM, K_α is related to the dislocation density and K_ε to the strain. In the above equation, the contribution from the film's grains is not taken into account, since in these films, the grain size exceeds 50 nm, as shown by SEM and AFM analysis. By plotting β_c vs. $\tan^2\theta$ and fitting the data to a linear least squares, the values for K_α and K_ε were obtained. K_α is related to the dislocation density N by

$$N = \frac{K_\alpha}{4.35b^2} \quad (2)$$

where b is the length of the Burger's vector. The dislocation density was calculated for one of the SrS:Ce,Sm films with the broadest rocking curve for the (002) peak (FWHM = 1.579°). For this film, the dislocation density was estimated from Eq. (2) to be 2×10^9 lines/cm^2, where the length of the Burger's vector was given by $a/\sqrt{2}$, and a is the lattice parameter of SrS (6.02203 Å). The strain for this sample is 0.05%. These results are summarized in Table 1. Notice that even at the optimized growth conditions, the SrS:Ce,Sm films have the broadest rocking curves of the three types of doped SrS films grown and are the only ones to show a measurable strain.

A ϕ-scan was obtained for a SrS:Eu,Sm sample with a very narrow rocking curve (FWHM = 0.307), using the SrS(224) reflection. In order to obtain the ϕ-scan, the detector was set at $2\theta = 77.622°$ and the angle between the diffraction vector and the surface normal was set at 3.55°. In this arrangement, $\phi = 0°$ corresponded to the MgO[010] edge being parallel to the X-ray beam. Fig. 5 shows the resulting ϕ-scan. These

Table 1
Summary of XRD analysis obtained for each of the three types of doped SrS films grown for this work, at their optimized growth conditions[a]

Sample	Deposition temperature (°C)	H_2S deposition pressure (mtorr)	Rocking curve FWHM (002)	$\langle a \rangle_{film}$ (Å)	Calculated strain
SrS:Eu,Sm	750	20	0.307°	6.0220 ± 0.0001	No strain
SrS:Ce,Sm	750	10	1.579°	6.0340 ± 0.0001	0.05%
SrS:Cu,Ge	800	10	0.220°	6.0223 ± 0.0001	No strain

[a]The bulk lattice constant for SrS is $\langle a \rangle_{bulk} = 6.022$ Å.

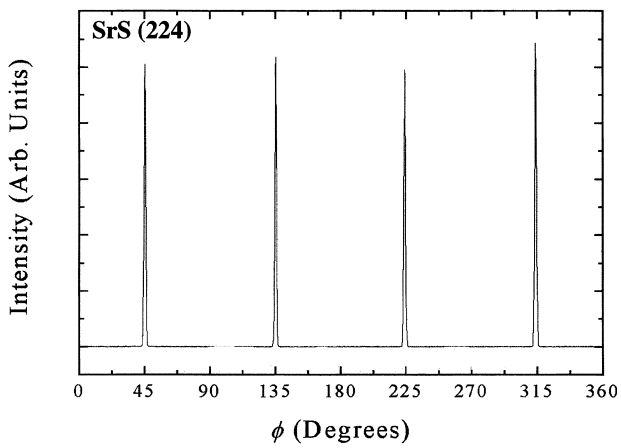

Fig. 5. X-ray ϕ-scans belonging to the SrS (111) peaks, from a SrS:Eu,Sm film. The position of these peaks indicates that the SrS film grows with its unit cell rotated in the plane by 45° with respect to the MgO unit cell.

results are indicative of the following epitaxial relationships:

[001] SrS || [001] MgO

(along the film normal), and

[100] SrS || [110] MgO

(in the plane of the film).

A θ–2θ scan of the SrS(224) reflection was also measured to obtain the in-plane lattice parameters. Using the (002), (004), (006) and (224) peak positions and applying the Riley–Nelson correction, the a and c lattice parameters were obtained assuming a tetragonal unit cell. Using this correction, the calculated lattice parameters for SrS are $a = 6.02203 \pm 0.0001$ Å and $c = 5.9794 \pm 0.0006$ Å. The in-plane c lattice parameter was closely related to the MgO lattice parameter ($\langle a \rangle_{MgO} = 4.213$ Å) by a factor of $\sqrt{2}$ ($\sqrt{2}\langle a \rangle_{MgO} = 5.958$ Å), consistent with the 45° rotation of the SrS lattice in reference to the MgO lattice. In this configuration, the lattice mismatch was calculated to be 0.35% with the SrS film under compression (lattice mismatch $= [a_s - a_f]/a_f$, where a_s and a_f are the substrate and film lattice parameters, respectively).

The thermally stimulated luminescence was evaluated for various SrS:Eu,Sm and SrS:Ce,Sm films. Prior comparisons between the TL glow curves from SrS:Eu,Sm films and bulk powders showed good agreement for those films with narrower rocking curves [11]. In the case of the SrS:Ce,Sm films, no correlation could be established between the film's rocking curve and their TL glow curves, but rather all the films showed glow curves similar to those obtained for the bulk SrS:Ce,Sm powders. Fig. 6 shows the TL glow curves from a SrS:Eu,Sm and a SrS:Ce,Sm film deposited at 750°C and 10 mtorr of H_2S. In the case of the SrS:Ce,Sm film, the TL peak appears near 90°C, indicating that its thermoluminescent behavior is dominated by the presence of shallow traps. For the SrS:Eu,Sm film, two TL peaks can be observed, one at ≈ 100°C and a second with higher intensity at ≈ 240°C. Luminescence at higher temperatures is desirable for optical storage applications, since it is indicative of the presence of more stable or deeper traps. For both samples, the intensity of the TL signal was quite high and demonstrates their potential use as direct replacements for powder phosphors for display applications.

4. Conclusions

This work has shown that high quality doped SrS films can be grown using PLD. Epitaxial films, free of particles or any other defects were deposited on MgO(001) substrates. Of the three types of doped SrS films made for this work, the SrS:Eu,Sm films showed the lowest rms surface roughness, approximately 2 nm. The deposition temperature and H_2S deposition pressure were found to affect the crystallinity of the films grown on MgO substrates, with the best results, as shown by XRD rocking curve analysis of the SrS (002) peak, obtained between 700 and 800°C and 10–20 mtorr for the three types of doped SrS coatings. For the SrS:Eu,Sm and SrS:Cu,Ge films no evidence of strain was detected and their lattice mismatch is only 0.35%. These results demonstrate that high quality doped SrS thin films with good luminescent properties can be grown by PLD. The brightness exhibited by the films in the TL measurements show the potential of these materials in thin film form for display applications.

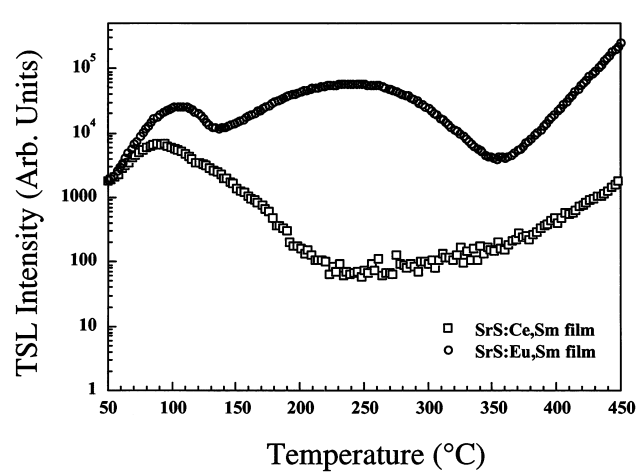

Fig. 6. Thermoluminescence emission corresponding to a SrS:Eu,Sm and a SrS:Ce,Sm thin films grown on MgO substrates by PLD. A 600-nm cut-off filter was used to block the black-body radiation.

Acknowledgements

The authors would like to thank S. Bounnak for her assistance with some of the depositions performed for this work. The authors would also like to thank B. Revay and B. Frazier of ETOM Technologies for providing the SrS:Eu,Sm and SrS:Ce,Sm targets; and S. Sun and C. King of Planar Systems for providing the SrS:Cu,Ge target. This work was supported by the Office of Naval Research.

References

[1] S. Jutamulia, G. Storti, J. Lindmayer, W. Seiderman, Proc. Soc. Photo-Opt. Instrum. Eng. 1151 (1990) 83.
[2] J. Lindmayer, Solid State Technol. 8 (1988) 135.
[3] C.N. King, J. Vac. Sci. Technol. A 14 (3) (1996) 1729.
[4] P.D. Rack, A. Naman, P.H. Holloway, S.-S. Sun, R.T. Tuenge, MRS Bull. 21 (3) (1996) 49.
[5] C. Karner, P. Maguire, J. MacLaughlin, S. Laverty, W.G. Graham, T. Morrow, R.M. Bowman, Phil. Mag. Lett. 76 (2) (1997) 111.
[6] K.O. Velthaus, U. Troppenz, B. Huettl, R. Herrmann, R. Mauch, Conference Record of the 1994 International Display Research Conference, Monterey, CA, (1994) 346.
[7] S. Albin, J.D. Satira, D.L. Livingston, T.A. Shull, Jpn. J. Appl. Phys. 31 (1) (1992) 715.
[8] W. Tong, Y.B. Xin, W. Park, C.J. Summers, Appl. Phys. Lett. 74 (1999) 1379.
[9] K. Neyts, G. Stuyven, Appl. Phys. Lett. 75 (1999) 2593.
[10] A. Piqué, R.C.Y. Auyeung, D.B. Chrisey, B. Justus, A. Houston, R.E. Revay, B. Frazier, Mater. Res. Soc. Symp. Proc. 508 (1998) 295.
[11] A. Piqué, M. Mathur, J. Moses, S.A. Mathews, Appl. Phys. Lett. 69 (1996) 391.